Journal of Sound and Vibration 327 (2009) 197–210

Contents lists available at ScienceDirect

Journal of Sound and Vibration

journal homepage: www.elsevier.com/locate/jsvi

The analysis of dynamic instability of a bimaterial beam with alternating magnetic fields and thermal loads

Guan-Yuan Wu *

Department of Fire Science, Central Police University, 56 Shu-jen Rd., Ta-kang, Kwei-san, Tao-yuan, 333 Taiwan, ROC

ARTICLE INFO

Article history:
Received 3 April 2008
Received in revised form
8 June 2009
Accepted 11 June 2009
Handling Editor: L.G. Tham
Available online 3 July 2009

ABSTRACT

In this study, the dynamic instabilities and transient vibrations of a bimaterial beam with alternating magnetic fields and thermal loads are investigated. Materials are assumed isotropic, and the physical properties are assumed to have unique values in each layer. Based on the Hamilton's principle, the equation of motion is derived in which the damping factor, the electromagnetic force, the electromagnetic torque, and the thermal load are considered. The solution of thermal effect is obtained by superposing certain fundamental linear elastic stress states which are compatible with Euler Bernoulli beam theory. Using the Galerkin's method, the equation of motion is reduced to a time-dependent Mathieu equation. The numerical results of the regions of dynamic instability are determined by the incremental harmonic balance (IHB) method, and the transient vibratory behaviors are presented by the fourth-order Runge–Kutta method. The results show that the responses of the dynamic instability and transient vibrations of the system are influenced by the temperature increase, the magnetic field, the thickness ratio, the excitation frequency, and the dimensionless damping ratio. The effects of using different values of parameters are presented to display the instability and steady vibrations and reveal some interesting characteristics such as beats and resonance phenomenon.

1. Introduction

Recently, the mechanics problems of electromagnet-mechanics of the structures have gained more importance in industrial application. Many researchers have paid their attention to the mechanical behavior of ferromagnetic structures such as beams, strips, plates, and shells [1–10]. One of the complicated problems of magneto-solids mechanics is how to treat the interaction of electromagnetic field with deformable structures.

In addition, thermal buckling or thermal effect may be an undesired phenomenon in many engineering. Temperature variations from a reference temperature may cause significant changes in the dynamic behavior of a structure, as temperature fields introduce thermal stress due to thermal expansion or contraction, and cause buckling of structures with two ends fixed [11,12]. Especially, it has long been known that structures constructed by bonding two or more materials and then subjected to temperature change, will be in a state of thermal stress [13,14]. Furthermore, the magnetic force and the temperature variation are interactive because temperature variation causes the value of the conductivity of magneto-elastic material to change. For a bimaterial pinned beam subjected to an alternating magnetic field and the thermal load, the thermal effect not only causes a state of thermal stress but also affects the dynamic behavior of the system. Therefore,

* Tel.: +886 3 318 5326; fax: +886 3 328 1114.
E-mail address: una210@mail.cpu.edu.tw

0022-460X/$ - see front matter © 2009 Elsevier Ltd. All rights reserved.
doi:10.1016/j.jsv.2009.06.012

the dynamic problem of a bimaterial beam associated with magneto-elastic material in the alternating magnetic field with thermal load is an interesting one and can be widely applied in engineering.

The first theoretical analysis of the problem of magneto-elastic buckling of a ferromagnetic plate in a transverse magnetic field was presented by Moon and Pao [15]. Based on the magnetic force on the distributed diploes and the quasi-static solution for the magnetization in the deformed plate, Moon and Pao obtained a mathematical mode of the critical magnetic field. Afterwards, much effort have been directed to develop mathematical models for studying the effect of magneto-elastic interactions upon static and dynamic behaviors of the magneto-elastic structures by taking into account the linear/nonlinear effect of deflections [16–21]. More recent advances are the smart or intelligent materials where piezoelectric and/or piezomagnetic materials are involved. For example, some intelligent structures with sensors and actuate of piezoelectric layers are designed to generate a damping such that the vibration of structures arisen from external disturbances is suppressed, or to modify the shape of an airfoil, thereby reducing transverse vortices [5,9]. Although, there is much research on modeling systems for the linear/nonlinear magnetization of structures, the work on the alternating transverse magnetic systems with the effect of thermal load is limited. Recently, the means of estimation of thermal effect in the oscillating magnetic field with linear/nonlinear thermoelastic relations has been developed by Wu [22,23]. For a small deflection, the results of instability carried out by the incremental harmonic balance (IHB) method in Ref. [22] have been identified to be good agreement with the results of Moon and Pao [16].

The aim of this study is to analyze the dynamic instabilities of a bimaterial beam subjected to an alternating magnetic field and thermal load with the linear strain. Materials are assumed isotropic, and the physical properties (the conductivity, the coefficient of thermal expansion and Young's modulus) are assumed to have unique values in each layer. The bimaterial beam made of magneto-elastic steel and silicon is applied to the theoretical model. As a result, the study presents formulas for the deformation and stress state in a bimaterial beam subjected to a temperature variation which varies linearly in the longitudinal direction. Again, the electromagnetic force and torque is arisen in one layer only.

In this study, the equation of motion is derived by Hamilton's principle in which the damping factor, induced current, and thermal load are considered simultaneously. The solution of thermal effect is obtained with the use of Euler Bernoulli beam theory, together with basic elements from the theory of elasticity. To obtain the solution in an analytical form, the assumed mode is employed. Using the Galerkin's method, the governing equation is reduced to a time-dependent Mathieu equation. The incremental harmonic balance method is adopted to determine the region of dynamic instability of the system by transforming the nonlinear governing equation into a set of linearized incremental algebraic equations in terms of Fourier coefficients, and solving by each incremental step. On the other hand, applying the fourth-order Runge–Kutta method, the transient vibrations are presented and discussed. The influences of the temperature variation, the magnetic field, the thickness ratio, the excitation frequency, and the dimensionless damping ratio on the dynamic response of this bimaterial beam system are investigated. In addition, the effects of using different values of excitation frequency, thickness ratio, and temperature increase to display the instability and steady vibrations are also presented and discussed.

2. Equation of motion

2.1. Statement of the problem

Consider the bimaterial beam of length L, width d and thickness h which pinned at its ends, as shown in Fig. 1. The beam consists of two different materials securely bonded to act as a single beam. Materials are assumed isotropic, and physical properties are assumed to have unique values in each layers. The thicknesses of the top and lower layers are denoted by h_t and h_l, respectively, while the total thickness of the beam is h. A Cartesian coordinate system is chosen such that the x–z plane is defined the neutral surface of the bimaterial beam, and the y–z plane is located at the left-hand end of the beam.

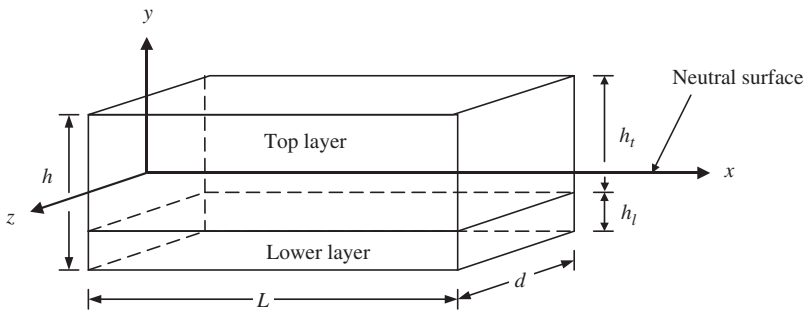

Fig. 1. Geometry and dimension of the bimaterial beam.

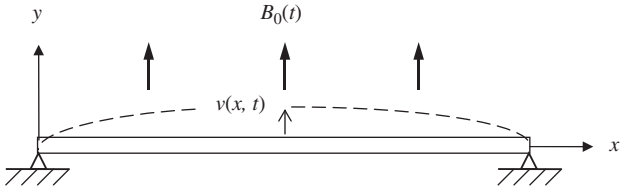

Fig. 2. The beam model.

An applied alternating uniform transverse magnetic field $B_0 = B_m \cos(\varpi \times t)\,\vec{j}$ and a uniform temperature increase ΔT cause a displacement (u, v) of the beam, where u and v are the longitudinal and transversal displacements, respectively (see Fig. 2). It is well noted that changes in temperature in an unconfined beam made of two-layer materials with different coefficients of thermal expansion (CTE) for each of the layers cause differential strains which give rise to internal thermal stresses and deformation. For simplicity of this problem, assuming that the width and thickness, compared to the length, is very small $(d, h \ll L)$. and the deflection is small. Thus, the beam is expected to deform according to Euler Bernoulli beam theory and be in a state of plane stress respecting the x–y plane.

2.2. Extended Hamilton's principle

The mathematical model of the elastic system can be obtained through the application of the integral of the Hamilton's principle, which assumes the following aspect:

$$\delta I_L = \int_{t_1}^{t_2} \delta(K + W - U)\,\mathrm{d}t + \int_{t_1}^{t_2} \delta W_c\,\mathrm{d}t = 0 \tag{1}$$

where K is the kinetic energy of the system, U is the potential energy, W is the work of externally applied force, and W_c is the work of nonconservative force. For a small deflection, the associated linear strain takes the form $\varepsilon_{xx} = \partial u/\partial x$, where u is the longitudinal displacement. The elastic strain energy caused by the increment ΔT has been expressed by the formulas [24]

$$U = \int_0^L EI2\left(\frac{\partial^2 v}{\partial x^2}\right)^2 \mathrm{d}x + \int_0^L \frac{A}{2E}[E\varepsilon_{xx} - \gamma(\Delta T)]^2\,\mathrm{d}x \tag{2}$$

where E is Young's modulus, I is the moment of inertia of the cross-section, A is the cross-section area, $\gamma(\Delta T)$ is the stress-temperature coefficient. In addition, the terms of K and W assume the following aspect:

$$\begin{aligned} K &= \frac{1}{2}\int_0^L m\left(\frac{\partial v}{\partial t}\right)^2 \mathrm{d}x \\ W_T &= \int_0^L c\frac{\partial v}{\partial x}\,\mathrm{d}x \\ W_P &= \int_0^L N(\mathrm{d}s - \mathrm{d}x) = \frac{1}{2}\int_0^L \left(\int_0^x p\,\mathrm{d}\xi\right)\left(\frac{\partial v}{\partial x}\right)^2 \mathrm{d}x \\ \delta W_c &= \int_0^L c_d\left(\frac{\partial v}{\partial t}\right)\delta v\,\mathrm{d}x \quad \text{and} \quad W = W_P + W_T \end{aligned} \tag{3}$$

where m is the mass of the beam per unit length, N is the axial compressive force of the beam, p is the body force of the beam per unit length, c is the body couple of the beam per unit length, and c_d is the damping ratio. Using the superposition principle, the total elastic strain energy of the bimaterial beam in this study can be shown as

$$U = \int_0^L \left(\frac{E_t I_t + E_l I_l}{2}\right)\left(\frac{\partial^2 v}{\partial x^2}\right)^2 \mathrm{d}x + \int_0^L \left\{\frac{A_t}{2E_t}[E_t\varepsilon_{xx} - \gamma_t(\Delta T)]^2 + \frac{A_l}{2E_l}[E_l\varepsilon_{xx} - \gamma_l(\Delta T)]^2\right\}\mathrm{d}x \tag{4}$$

where the subscripts t and l refer to values calculated for the top and lower layers of the beam, respectively. The I_t and I_l are the moments of inertia of the top and lower layers about the neutral axis of the beam.

Eq. (1) can be written as

$$\begin{aligned}\delta I_L = &\int_{t_1}^{t_2}\int_0^L \left\{ m\frac{\partial^2 v}{\partial t^2} + \frac{\partial c}{\partial x} + \frac{\partial}{\partial x}\left[\left(\int_0^x p\,\mathrm{d}\xi\right)\frac{\partial v}{\partial x}\right] + (E_tI_t + E_lI_l)\frac{\partial^4 v}{\partial x^4}\right\} \\ &- E_tA_t\frac{\partial}{\partial x}\left\{\left[\frac{\partial u}{\partial x} - \frac{\gamma_t(\Delta T)}{E_t}\right]\frac{\partial v}{\partial x} - E_lA_l\frac{\partial}{\partial x}\left\{\left[\frac{\partial u}{\partial x} - \frac{\gamma_l(\Delta T)}{E_l}\right]\frac{\partial v}{\partial x}\right\}c_d\frac{\partial v}{\partial t}\right\}\delta v\,\mathrm{d}x\,\mathrm{d}t \\ &+ \int_{t_1}^{t_2}\left\{(E_tI_t + E_lI_l)\frac{\partial^2 v}{\partial x^2}\frac{\partial}{\partial x}(\delta v) - (E_tI_t + E_lI_l)\frac{\partial^3 v}{\partial x^3}\delta v - c\delta v - \left(\int_0^x p\,\mathrm{d}\xi\right)\frac{\partial v}{\partial x}\delta v\right. \\ &\left. + \left\{E_tA_t\left[\frac{\partial u}{\partial x} - \frac{\gamma_t(\Delta T)}{E_t}\right] + E_lA_l\left[\frac{\partial u}{\partial x} - \frac{\gamma_l(\Delta T)}{E_l}\right]\right\}\frac{\partial v}{\partial x}\delta v\right\}\Big|_0^L \mathrm{d}t \\ &- \int_{t_1}^{t_2}\int_0^L\left\{E_tA_t\frac{\partial}{\partial x}\left[\frac{\partial u}{\partial x} - \frac{\gamma_t(\Delta T)}{E_u}\right] + E_lA_l\frac{\partial}{\partial x}\left[\frac{\partial u}{\partial x} - \frac{\gamma_l(\Delta T)}{E_l}\right]\right\}\delta u\,\mathrm{d}x\,\mathrm{d}t \\ &+ \int_{t_1}^{t_2}\left\{E_tA_t\left[\frac{\partial u}{\partial x} - \frac{\gamma_t(\Delta T)}{E_t}\right] + E_lA_l\left[\frac{\partial u}{\partial x} - \frac{\gamma_l(\Delta T)}{E_l}\right]\right\}\delta u\Big|_o^L \mathrm{d}t - \int_0^L\left(m\frac{\partial v}{\partial t}\delta v\right)\Big|_{t_1}^{t_2}\mathrm{d}x = 0 \end{aligned} \tag{5}$$

For a pinned supported beam, the deflections and the bending moments at both ends are zero; hence the boundary conditions are assumed that

$$\delta u(0) = \delta u(L) = \delta v(0) = \delta v(L) = 0$$

$$v(0) = v(L) = 0 \quad \text{and} \quad \partial^2 v/\partial x^2 = 0 \quad \text{at } x = 0 \text{ and } L \tag{6}$$

In order to maintain consistency with the boundary conditions, the total strain of the two layers is zero (no displacement) at both ends of the beam. The equilibrium equations can be obtained

$$E_tA_t\frac{\partial}{\partial x}\left[\frac{\partial u}{\partial x} - \frac{\gamma_t(\Delta T)}{E_t}\right] = E_lA_l\frac{\partial}{\partial x}\left[\frac{\partial u}{\partial x} - \frac{\gamma_l(\Delta T)}{E_l}\right] = 0 \tag{7}$$

$$\begin{aligned} &m\frac{\partial^2 v}{\partial t^2} + c_d\frac{\partial v}{\partial t} + (E_tI_t + E_lI_l)\frac{\partial^4 v}{\partial x^4} + \frac{\partial c}{\partial x} + \frac{\partial}{\partial x}\left[\left(\int_0^x p\,\mathrm{d}\xi\right)\frac{\partial v}{\partial x}\right] \\ &- E_tA_t\frac{\partial}{\partial x}\left\{\left[\frac{\partial u}{\partial x} - \frac{\gamma_t(\Delta T)}{E_t}\right]\frac{\partial v}{\partial x} - E_lA_l\frac{\partial}{\partial x}\left\{\left[\frac{\partial u}{\partial x} - \frac{\gamma_l(\Delta T)}{E_l}\right]\frac{\partial v}{\partial x}\right\} = 0 \end{aligned} \tag{8}$$

Eq. (7) will be satisfied assuming

$$\frac{\partial u}{\partial x} - \frac{\gamma_t(\Delta T)}{E_t} = \frac{\partial u}{\partial x} - \frac{\gamma_l(\Delta T)}{E_l} = \text{constant} = \bar{\delta}(\Delta T) \tag{9}$$

where $\bar{\delta}(\Delta T)$ is equal to the average strain of the system. Thus, the following conditions must be enforced:

$$\begin{aligned}\bar{\delta}(T) &= \frac{1}{L}\int_0^L\left[\frac{\partial u}{\partial x} - \frac{\gamma_t(\Delta T)}{E_t}\right]\mathrm{d}x = \frac{1}{L}\int_0^L\left[\frac{\partial u}{\partial x} - \frac{\gamma_l(\Delta T)}{E_l}\right]\mathrm{d}x \\ &= -\frac{\gamma_t(\Delta T)}{E_t} = -\frac{\gamma_l(\Delta T)}{E_l}\end{aligned} \tag{10}$$

Substituting Eq. (10) into Eq. (8), the equation of motion is derived as

$$m\frac{\partial^2 v}{\partial t^2} + c_d\frac{\partial v}{\partial t} + (E_tI_t + E_lI_l)\frac{\partial^4 v}{\partial x^4} + \frac{\partial c}{\partial x} + \frac{\partial}{\partial x}\left[\left(\int_0^x p\,\mathrm{d}\xi\right)\frac{\partial v}{\partial x}\right] + [A_t\gamma_t(\Delta T) + A_l\gamma_l(\Delta T)]\frac{\partial^2 v}{\partial x^2} = 0 \tag{11}$$

3. Analytical procedure

3.1. Electromagnetic force **F** and torque **c**

For the pinned beam, the displacement function can be written as

$$v(x,t) = \sum_{n=1,2,\ldots} w_n(t)\sin\lambda_n x, \quad 0 \le x \le L \tag{12}$$

where $\lambda_1 = \pi/L$ for the first mode.

Based on a small deflection and linear elastic assumptions, the electromagnetic force **F** and torque **c** arising from an alternating uniform transverse magnetic field which acts on a symmetric cross-section beam of thickness h_b, width d, and

length L have been derived by Shih et al. [2] and Wu [22] as follows:

$$\mathbf{F} = p\vec{i} = \sum_{n=1,2,\ldots} \left(\frac{\sigma}{4}\right)\lambda_n^2 h_b \, \mathrm{d}B_m^2 \left[x + \left(\frac{\lambda_n}{2}\right)\sin 2\lambda_n x\right](1+\cos 2\varpi t) w_n \dot{w}_n \vec{i} \tag{13}$$

$$\mathbf{c} = \sum_{n=1,2,\ldots} \lambda_n \Phi_n d \cos\lambda_n x (1+\cos 2\varpi t) w_n \vec{k} \tag{14}$$

where σ is the conductivity of the material, μ_0 is the permeability of the vacuum, μ_r is the relative permeability, and $\Phi_n = \chi^2 B_m^2 \sinh(\lambda_n h_b/2)/(\mu_0 \mu_r \lambda_n \Delta_n)$, $\chi = 1-\mu_r$ is the susceptibility, and $\Delta_n = \mu_r \sinh(\lambda_n h_b/2) + \cosh(\lambda_n h_b/2)$.

Substituting Eqs. (12)–(14) into Eq. (11) leads to a linear operator $\Pi(w)$

$$\begin{aligned}\Pi(w) = \sum_{n=1,2\ldots} \Bigg\{ \Bigg\{ & m\ddot{w}_n + c_d \dot{w}_n - \lambda_n^2 \Phi_n d(1+\cos 2\varpi t) w_n + (E_t I_t + E_l I_l)\lambda_n^4 w_n \\ & - [A_t \gamma_t(\Delta T) + A_l \gamma_l(\Delta T)]\lambda_n^2 w_n \} \sin\lambda_n x \\ & - \left(\frac{\sigma}{4}\right)\lambda_n^3 h_b \, \mathrm{d}B_m^2 (1+\cos 2\varpi t) w_n^2 \dot{w}_n \Bigg\{ \lambda_n \left[\frac{x^2}{2} + \frac{1}{4\lambda_n^2}(1-2\cos 2\lambda_n x)\right] \\ & \times \sin\lambda_n x - \left(x + \frac{1}{2\lambda_n}\sin 2\lambda_n x\right)\cos\lambda_n x \Bigg\} \Bigg\} = 0 \end{aligned} \tag{15}$$

3.2. Temperature effects

3.2.1. The conductivity

The conductivity σ of a material, is simply reciprocal of its resistivity, so $\sigma = 1/\vartheta$, where ϑ is the resistivity of the material. In addition, the temperature and resistivity of material are dependent, since they are related by the relation

$$\vartheta = \vartheta_0 + \vartheta_0 \alpha_r \Delta T \tag{16}$$

where ϑ_0 is the resistivity at room temperature and α_r is the temperature coefficient of resistivity.

3.2.2. The neutral surface and moment of inertia

The solutions consider the top and the lower layers as separate ones subjected to the temperature increase ΔT. Since each layer has unique coefficient of thermal expansion, the resulted axial displacements $\delta_t^{th}(x)$ and $\delta_l^{th}(x)$ at distance x are

$$\delta_t^{th}(x) = \alpha_t \Delta T x \quad \text{and} \quad \delta_l^{th}(x) = \alpha_l \Delta T x \tag{17}$$

where α is the coefficient of thermal expansion. In this study, the deformations of the two layers must be compatible ultimately. An addition set of elastic displacements, $\delta_t^e(x)$ and $\delta_l^e(x)$, must be imposed such that

$$\delta_t^{th} + \delta_t^e = \delta_l^{th} + \delta_l^e \tag{18}$$

One considers the coefficient of thermal expansion of the lower layer is greater than the top layer of the beam ($\alpha_l > \alpha_t$). The axial forces existing in the top layer and lower layer in the original assembly must result in deflection compatibility at the end of the beam such that they stretch the top layer and shorten the lower layer until the final elongations of the two layers are the same i.e. the axial force P_f acts to the outside direction on the top beam and to the inside direction on the lower beam. Therefore, the axial elastic displacement of the beam in each layer can be shown as

$$\delta_t^e(x) = \frac{P_f x}{E_t A_t} \quad \text{and} \quad \delta_l^e = -\frac{P_f x}{E_l A_l} \tag{19}$$

Substituting Eqs. (17) and (19) into Eq. (18), the magnitude of the axial force P_f can be determined,

$$P_f = \frac{(\alpha_l - \alpha_t)\Delta T \, \mathrm{d} E_l h_l E_t h_t}{E_t h_t + E_l h_l} \tag{20}$$

In order to maintain consistency with Euler Bernoulli beam theory, the axial force P_f is equal to the bending moment M_t and M_l which act on the ends of the bimaterial beam as shown in Fig. 3. Thus the following condition can be obtained:

$$M_t + M_l - \frac{P_f(h_t + h_l)}{2} = 0 \tag{21}$$

If the material beam is linearly elastic and follows Hooke's law, the curvature k is

$$k = \frac{1}{r_r} = \frac{M_t}{E_t I_t} = \frac{M_l}{E_l I_l} \tag{22}$$

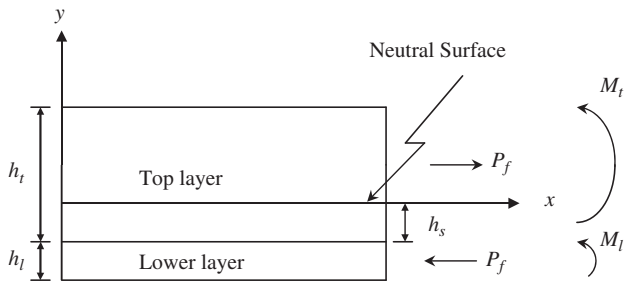

Fig. 3. Forces and moments on the bimaterial beam element.

where r_r is the radius of curvature. Using the parallel-axis theorem, the I_t and I_l can be written as

$$I_t = \frac{\mathrm{d}h_t^3}{12} + \mathrm{d}h_t\left(\frac{h_t}{2} - h_s\right)^2, \quad I_l = \frac{\mathrm{d}h_l^3}{12} + \mathrm{d}h_l\left(\frac{h_l}{2} + h_s\right)^2 \tag{23}$$

where h_s denotes the distance from the top of the lower layer to the neutral surface. To obtain the h_s, we can use the zero net axial force at the ends of the beam so that $\int \sigma_t \,\mathrm{d}A + \int \sigma_l \,\mathrm{d}A = 0$. Then the calculation is

$$\int_{-d/2}^{d/2}\int_{-h_s}^{h_t-h_s} E_t\left(\frac{1}{r_r}\right) y \,\mathrm{d}y\,\mathrm{d}z + \int_{-d/2}^{d/2}\int_{-(h_l+h_s)}^{-h_s} E_l\left(\frac{1}{r_r}\right) y \,\mathrm{d}y\,\mathrm{d}z = 0 \tag{24}$$

Therefore, the result of h_s is

$$h_s = \frac{E_t h_t^2 - E_l h_l^2}{2(E_t h_t + E_l h_l)} \tag{25}$$

3.2.3. The stress-temperature coefficients

As mentioned previously, if the beam is subjected to an amount of temperature change ΔT without axial restraint, the elongation will simply be an expansion in length of δ. The displacement can be derived by Eq. (18), and shown as

$$\delta = \delta_t = \delta_l = \frac{P_f L}{E_t A_t} + \alpha_t \Delta T L = -\frac{P_f L}{E_l A_l} + \alpha_l \Delta T L \tag{26}$$

Considering an axial restraint beam, the total displacement δ becomes zero (but not stress free) on the ends of the beam. Assuming that the thermal expansion is vanished to opposite contraction by the restraining force P_h^*, the magnitude of the P_h^* can be shown as

$$P_h^* = P_t + P_l \tag{27}$$

where P_t and P_l are the restraint forces for the top and lower layers, respectively. Now, the beam is no displacement, and then the axial restraint force is equal to $-EA\varepsilon$. The yield P_t, and P_l are,

$$P_t = -(\alpha_t E_t A_t \Delta T + P_f) \quad \text{and} \quad P_l = -(\alpha_l E_l A_l \Delta T - P_f) \tag{28}$$

Ultimately, the thermal expansion is canceled out by equal and opposite contraction caused by the restraining force, due to the total strain is zero for both ends. Therefore, the stress-temperature coefficients in each layer are

$$\gamma_t(\Delta T) = E_t \alpha_t \Delta T + \frac{P_f}{A_t}, \quad \gamma_l(\Delta T) = E_l \alpha_l \Delta T - \frac{P_f}{A_l} \tag{29}$$

3.3. Galerkin's method

In this study, the first mode ($n = 1$) is considered, which means $\lambda = \pi/L$. Taking $\sin \lambda x$ as the base function, Galerkin's equation leads to

$$\int_0^L \Pi(w) \sin\,\lambda x \,\mathrm{d}x = 0 \tag{30}$$

By simplifying Eq. (30), a time-dependent differential equation is derived as follows:

$$\frac{d^2w}{dt^2}+2[k+\varsigma(1+\cos 2\varpi t)w^2]\frac{dw}{dt}+(\omega_L^2-\xi\cos 2\varpi t)w=0 \tag{31}$$

where ρ_t and ρ_l are the density of the top and lower layers, respectively,

$$2\kappa=\frac{c_d}{(\rho_t h_t+\rho_l h_l)d},\quad 2\varsigma=\frac{\sigma h_b B_m^2\lambda^2(-4\lambda^2L^2-9)}{48(\rho_t h_t+\rho_l h_l)},\quad \omega_0^2=\frac{(E_tI_t+E_lI_l)\lambda^4}{(\rho_t h_t+\rho_l h_l)d}$$

$$\omega_L^2=\omega_0^2\left(1-\frac{B_r^2}{B_c^2}-\frac{A_t\gamma_t(\Delta T)+A_l\gamma_l(\Delta T)}{P_c}\right),\quad B_r^2=\frac{B_m^2}{2},\quad P_c=(E_tI_t+E_lI_l)\frac{\pi^2}{L^2}$$

$$B_c^2=\frac{(E_tI_t+E_lI_l)\lambda^3\mu_0\mu_r\Delta}{2\chi^2 d\,\sinh\dfrac{\lambda h_l}{2}},\quad \xi=\frac{\Phi\lambda^2}{\rho_t h_t+\rho_l h_l}\quad\text{and}\quad \sigma=\frac{1}{\vartheta_0+\vartheta_0\alpha_r\Delta T}$$

The new parameter are defined as $\Omega=\varpi/\omega_L$, $\tau=\varpi t$, $k_1=\kappa/\omega_L$, $k_2=\varsigma/\omega_L$, and $2\varphi=\xi/\omega_L^2$. Eq. (31) is simplified to well-known Mathieu equation:

$$\Omega^2\frac{d^2w}{d\tau^2}+2\Omega[k_1+k_2(1+\cos 2\tau)w^2]\frac{dw}{d\tau}+(1-2\varphi\cos 2\tau)w=0 \tag{32}$$

3.4. The IHB formulation

In the recent decades, the IHB method has been successfully applied to various types of nonlinear dynamics problems. The procedure of the IHB method used to solve Eq. (32) is mainly divided into two steps. The first step is a Newton–Raphson procedure. The second step is to find an approximate solution by assuming a periodic solution and applying Galerkin's method.

The current state of vibration corresponding to a point (Ω_0,φ_0) on instability boundary is denoted by w_0. A neighboring state is reached through a parameter incrementation:

$$\varphi=\varphi_0+\Delta\varphi,\quad \Omega=\Omega_0+\Delta\Omega,\quad w=w_0+\Delta w \tag{33}$$

Substituting Eq. (33) into Eq. (32) and neglecting the nonlinear terms of $\Delta\varphi$, $\Delta\Omega$, Δw, a linearized incremental equation is obtained:

$$\begin{aligned}&\Omega_0^2\Delta\ddot{w}+2\Omega_0[k_1+k_2(1+\cos 2\tau)w_0^2]\Delta\dot{w}+(1-2\varphi_0\cos 2\tau)\Delta w+4\Omega_0k_2(1+\cos 2\tau)w_0\Delta w\Delta\dot{w}\\&\quad=R+2\Delta\varphi w_0\cos 2\tau-2\Delta\Omega\Omega_0\ddot{w}_0-2\Delta\Omega[k_1+k_2(1+\cos 2\tau)w_0^2]\dot{w}_0\end{aligned} \tag{34a}$$

where

$$R=-\{\Omega_0^2\ddot{w}_0+2\Omega_0[k_1+k_2(1+\cos 2\tau)w_0^2]\dot{w}_0+(1-2\varphi_0\cos 2\tau)w_0\} \tag{34b}$$

The approximate functions w_0 and Δw can be expanded into a truncated Fourier series,

$$w_0(\tau)=\sum_{k=1,3,\ldots}^{2N-1}(a_k\sin k\tau+b_k\cos k\tau)\quad\text{and}\quad \Delta w(\tau)=\sum_{k=1,3,\ldots}^{2N-1}(\Delta a_k\sin k\tau+\Delta b_k\cos k\tau) \tag{35}$$

for the principal region of instability, corresponding to a solution of period 2π. N is the number of temporal terms for calculation.

Substituting (35) into (34a) and using the Galerkin's procedure, a set of linear equations can be obtained as follows:

$$[C]\{\Delta a\}=\{R\}+\Delta\varphi\{P\}+\Delta\Omega\{Q\} \tag{36}$$

where $[C]$ is the matrix for the Fourier coefficients and $\{\Delta a\}$ is a vector consisting of Fourier coefficients Δa_k or Δb_k, for example: $\{\Delta a\}^T=\{\Delta a_1,\Delta a_3,\Delta a_5,\ldots\}$. $\{R\}$ is the corrective vector derived from (34b), and $\{P\}$, $\{Q\}$ are vectors obtained from the second and third right-hand side terms, respectively.

In Eq. (36), a linear system of $2N$ equations with $2N$+2 unknowns Δa, $\Delta\varphi$ and $\Delta\Omega$ has to be solved at each incremental step. Hence, it is necessary to add two constraints among Δa, $\Delta\varphi$, and $\Delta\Omega$. The corresponding procedures used to solve Eq. (36) and to determine the unknowns are discussed in Refs. [25–27].

4. Numerical results and discussions

Numerical simulations are presented for the dynamic instabilities and transient vibrations of a bimaterial pinned beam subjected to a uniform alternating transverse magnetic field and thermal load. The bimaterial beam is composed of a lower

layer beam made from magneto-elastic steel and a top layer beam made from silicon. The material application implies that when the beam is in impulsion magnetic field, the electromagnetic force and torque is arisen in the lower layer only. In addition, materials in the lower layer and in the top layer are homogeneous and isotropic, but the coefficients of linear thermal expansion are different, where $\alpha_l > \alpha_t$. The physical parameters of this system are given as

$L = 0.4\,\text{m}$, $h = 5 \times 10^{-3}\,\text{m}$, $d = 2 \times 10^{-2}\,\text{m}$, $E_l = 1.94 \times 10^{11}\,\text{Pa}$, $\rho_l = 7930\,\text{kg/m}^3$, $\alpha_l = 11 \times 10^{-6}\,^\circ\text{C}^{-1}$, $\mu_r = 3.0 \times 10^3$, $\mu_0 = 1.26 \times 10^{-6}\,\text{H/m}$, $\alpha_r = 6.5 \times 10^{-3}\,^\circ\text{C}^{-1}$, $\vartheta_0 = 9.68 \times 10^{-8}\,\Omega\,\text{m}$ (ohm-meter), $E_t = 1.72 \times 10^{11}\,\text{Pa}$, $\rho_t = 2330\,\text{kg/m}^3$, $\alpha_t = 2.5 \times 10^{-6}\,^\circ\text{C}^{-1}$.

4.1. Dynamic instability response

In order to gain further insight into various thermal loads of the bimaterial beam and to show the effects of the magnetic fields on the dynamic responses of the excited beam, numerical results of the solution were performed a wide variety of parameters. Now one considers damping parameter $k_1 = 0$ and thickness ratio $h_t/h_l = 1.0$, then different temperature increases are applied. The effect of temperature increase ΔT on the principal instability region is shown in Fig. 4. It can be seen from the presented regions that increasing temperature shifts the region to a lower value and produces a large variety of responses. In this study, the fundamental frequency ω_L varying with a magnetic field and an increased temperature can be obtained by Eq. (31), while $[B_r^2/B_c^2 + (A_t\gamma_t + A_l\gamma_l)\Delta T/P_c] < 1$. It displays that, just as the theory predicted, a higher temperature increase results to a lower natural frequency for this system. While $B_m = 0.3\,\text{T}$, $h_t/h_l = 1.0$ and $\Delta T = 3.0\,^\circ\text{C}$, the points A, B, and C are 470.0, 463.3, and 450.0 rad/s, respectively, and are located in the principal instability region. These points corresponding to the time responses will be discussed and shown in the next section. The effects of varying thickness ratio h_t/h_l on the principal instability regions associated with different temperature increases are illustrated in Figs. 5 and 6. As it can be seen, the increase in the thickness ratio h_t/h_l of the bimaterial beam has the beneficial effect on increasing the value of natural frequency. If the pinned beam is considered with uniform thickness and material is assumed to be isotropic, the natural frequency of the beam made from the top layer material silicon is higher than that of the lower layer material low-carbon steel. It is in accordance with Fig. 6 that the higher thickness ratio results to the higher fundamental natural frequency of this system. Fig. 7 shows the regions of dynamic instability for different damping coefficients k_1 for $h_t/h_l = 1.0$ and $\Delta T = 0$. It shows that an increase in damping coefficient results in a reduction of the region of instability. On the other hand, it can be considered that when viscous damping is included, a least magnitude of the magnetic field is required to make the dynamic instability of the system.

4.2. The part of vibration

In order to analyze the transient vibration characteristics of this system, the fourth-order Runge–Kutta method is applied to solve Eq. (31) by the step size of 2.0×10^{-5}. The initial conditions are chosen as $dw/dt = 0$, $w/h = 1.0$, and $c_d = 0.05$.

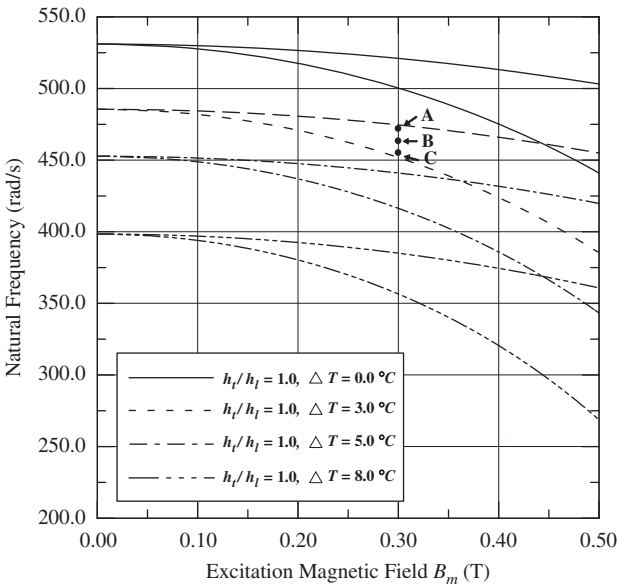

Fig. 4. The effect of temperature increase ΔT on the principal parametric instability regions for the thickness ratio $h_t/h_l = 1.0$.

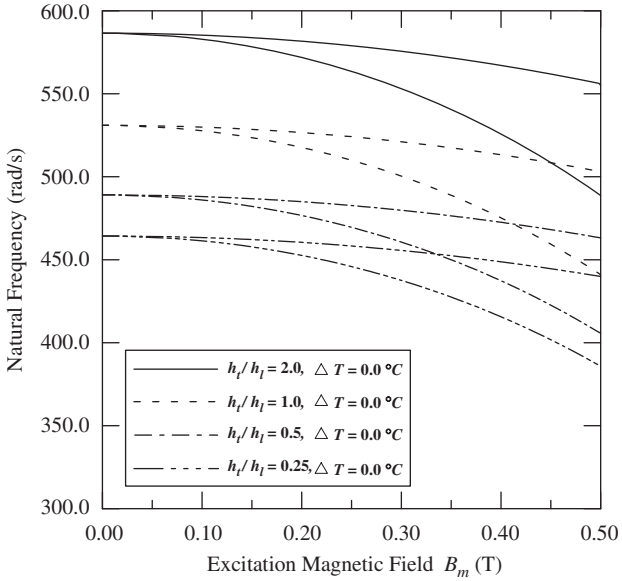

Fig. 5. The effect of varying thickness ratio h_t/h_l on the principal parametric instability regions without temperature increase.

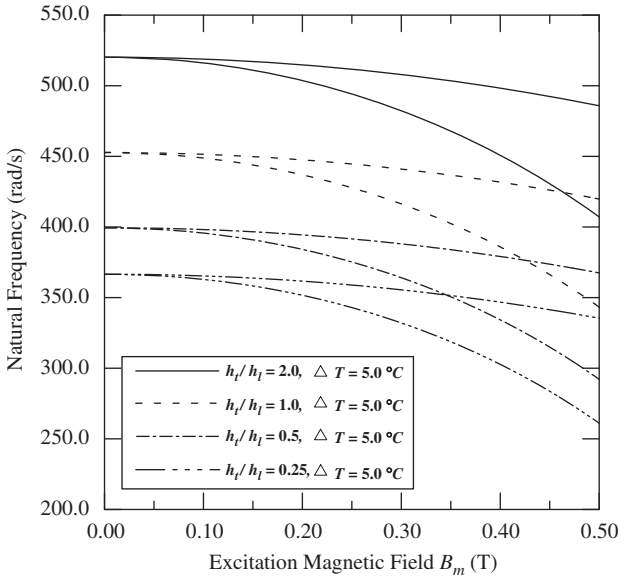

Fig. 6. The effect of varying thickness ratio h_t/h_l on the principal parametric instability regions with temperature increase $\Delta T = 5.0\,^{\circ}\mathrm{C}$.

While $h_t/h_l = 1.0$, $\varpi = 80.0\,\mathrm{rad/s}$, and $\Delta T = 0$, the result of amplitude versus time associated with different magnetic fields ($B_m = 0.1, 0.3, 0.5\,\mathrm{T}$ (tesla)) is shown in Fig. 8. In this case, assuming that $\Delta T = 0$, the restraint force P_h^* and the stress-temperature coefficient $\gamma(\Delta T)$ will be zero as well, i.e., the thermal expansion of the system has no contribution to the axial force. The changes of this nonlinear vibration are determined by the magnetic field only. For the same beam, the increase temperature, ΔT is replaced by 1.0, 3.0, and 5.0 °C, respectively. The result of the nonlinear vibration is shown in Fig. 9. It can be seen from these presented waveforms that either increasing the magnetic field or the temperature shifts the frequency of the nonlinear system to a lower value, i.e., increasing the period of the nonlinear vibration system. Fig. 10 shows that the effect of different thickness ratios on the system, while $B_m = 0.1\,\mathrm{T}$, $\varpi = 80.0\,\mathrm{rad/s}$ and $\Delta T = 3.0\,^{\circ}\mathrm{C}$. The results show that the increase of the thickness ratio decreases the frequency of the system. It should be noted that the fundamental frequency of this system corresponding to the magnetic field, the temperature increase, and the thickness ratio can be obtained through the relation $\omega_L^2 = \omega_0^2 \times (1 - B_r^2/B_c^2 - [A_t\gamma_t(\Delta T) + A_l\gamma_l(\Delta T)]/P_c)$. In addition, because the small deflection is assumed, the effect of nonlinear damping ς on the region of instability is insignificant as discussed in Ref. [22].

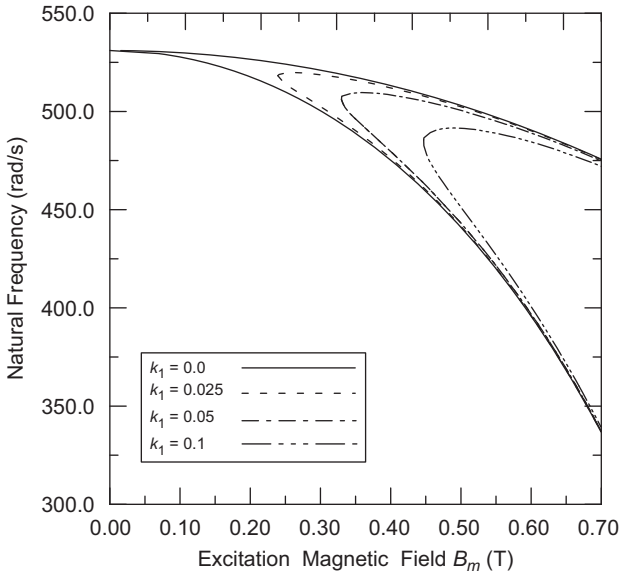

Fig. 7. The influence of damping on the principal parametric instability regions for $h_t/h_l = 1.0$ and $\Delta T = 0$.

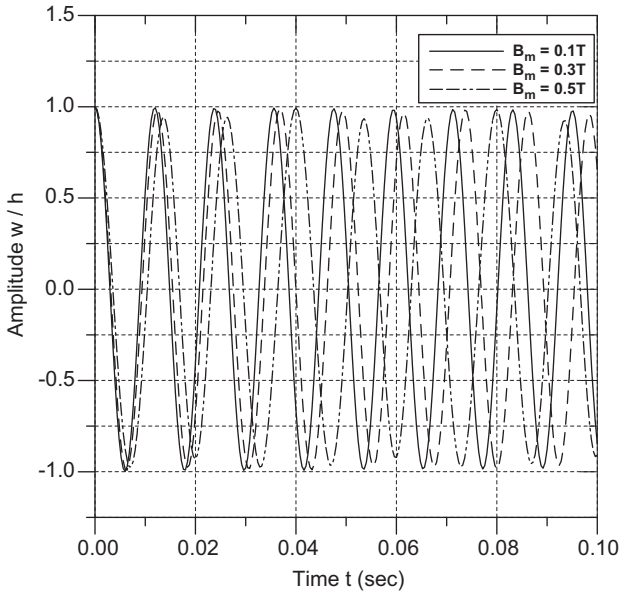

Fig. 8. The relationship of amplitude and time for $h_t/h_l = 1.0$ and $\Delta T = 0$ with different values of the magnetic field.

While $k_1 = 0$, $h_t/h_l = 1.0$, $\Delta T = 3.0\,^{\circ}\mathrm{C}$ and $B_m = 0.3\,\mathrm{T}$ are applied, the fundamental frequency of the system becomes 463.28 rad/s. We now consider the cases that the excitation frequency approaches the natural frequency of this system. Figs. 11 and 12 represent the results of waveforms, when the excitation frequency ϖ is applied by 80.0 (out of the region), 470.0 (point A, top boundary of the region), 463.3 (point B, in the region), and 457.0 (point C, lower boundary of the region) rad/s, individually. It is well known that when the ratio of the excitation frequency with respect to the natural frequency of the system closes to 1.0, the primary region of the dynamic instability occurs, and the intensity of beats decreases appreciably as the lower boundary of the region of exciting is approached [28]. The values of the excitation frequency $\varpi = 457.0$ (point C) and 470.0 (point A) rad/s are located on the lower and the top boundary of the instability region of this system, respectively, and the excitation frequency $\varpi = 463.3$ (point B) rad/s is equal to the natural frequency. As can be seen from these waveforms, the beat phenomenon occurs for $\varpi = 457.0$ and 470.0 rad/s, and the resonance phenomenon occurs for $\varpi = 463.3$ rad/s. Therefore, the beat and resonance phenomenon of this system agree with the theory prediction.

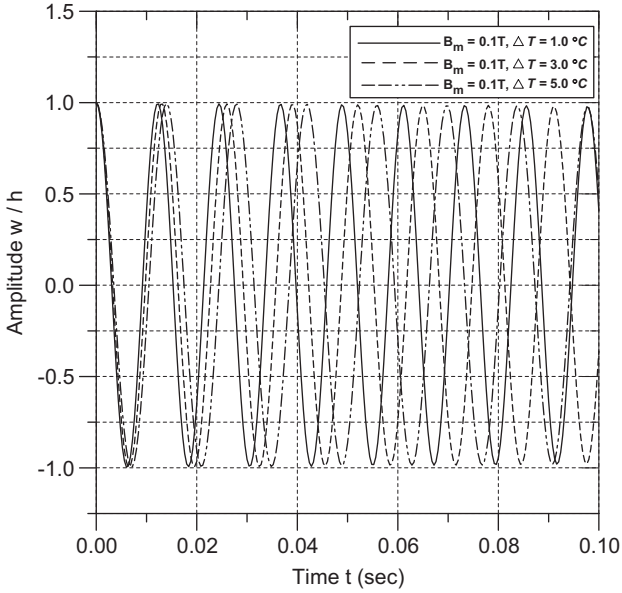

Fig. 9. The relationship of amplitude and time for $h_t/h_l = 1.0$ and $B_m = 0.1\,\mathrm{T}$ with different values of the temperature increase.

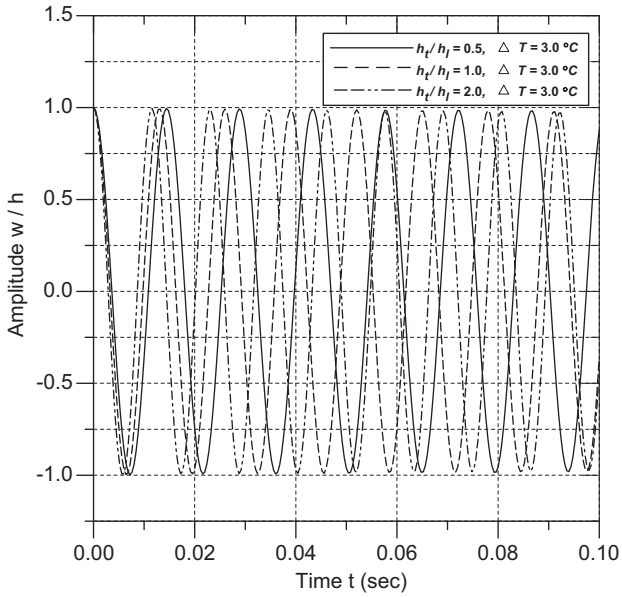

Fig. 10. The relationship of amplitude and time for $B_m = 0.1\,\mathrm{T}$ and $\Delta T = 3.0\,^{\circ}\mathrm{C}$ with different values of the thickness ratio.

We now consider the case that the magnetic field has a fixed excitation frequency to the system. While $B_m = 0.3\,\mathrm{T}$, $h_t/h_l = 1.0$, $\Delta T = 3.0\,^{\circ}\mathrm{C}$ and $\varpi = 463.3\,\mathrm{rad/s}$ are applied, the results of maximum amplitudes and minimum amplitudes versus time associated with different thickness ratios and different temperature increases are shown in Figs. 13 and 14, respectively. As mentioned above, the natural frequency of the beam made from the top layer material silicon is higher than that of the lower layer material low-carbon steel. Therefore, it is realized that increasing the thickness ratio h_t/h_l or decreasing the temperature increase ΔT leads to the higher value of the fundamental natural frequency. In addition, though $\varpi = 463.3\,\mathrm{rad/s}$ is equal to the fundamental natural frequency of the initial system, the transient vibration is obviously affected by the changes of the temperature increase or thickness ratio. It is worth mentioning that when $h_t/h_l = 1.5$ or $\Delta T = 0.0\,^{\circ}\mathrm{C}$, the maximum and minimum amplitude is continuous 1.0 and -1.0, respectively, i.e., the vibration is steady. In fact, the results show that the principal regions of dynamic instability of these two cases ($h_t/h_l = 1.5$ or $\Delta T = 0.0\,^{\circ}\mathrm{C}$) are far away from that of the initial conditions.

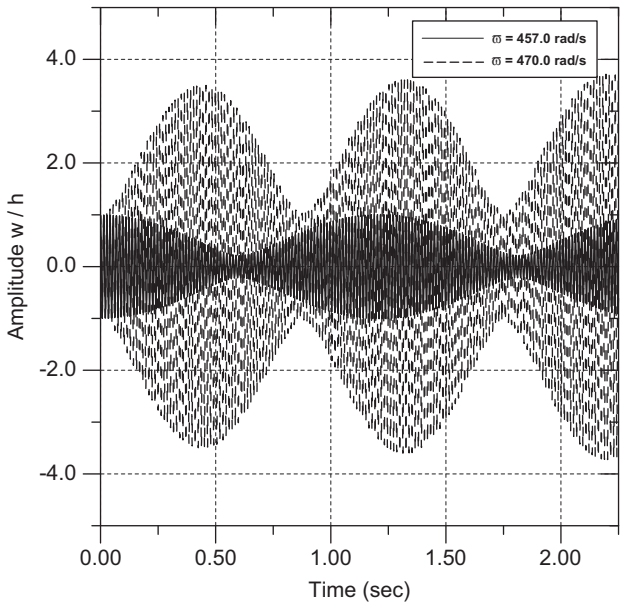

Fig. 11. The relationship of amplitude and time of the system ($k_1 = 0$, $h_t/h_l = 1.0$, $\Delta T = 3.0\,^{\circ}\mathrm{C}$ and $B_m = 0.3\,\mathrm{T}$) corresponding to different values of the excitation frequency ($\varpi = 457.0\,\mathrm{rad/s}$, point C and $470.0\,\mathrm{rad/s}$, point A).

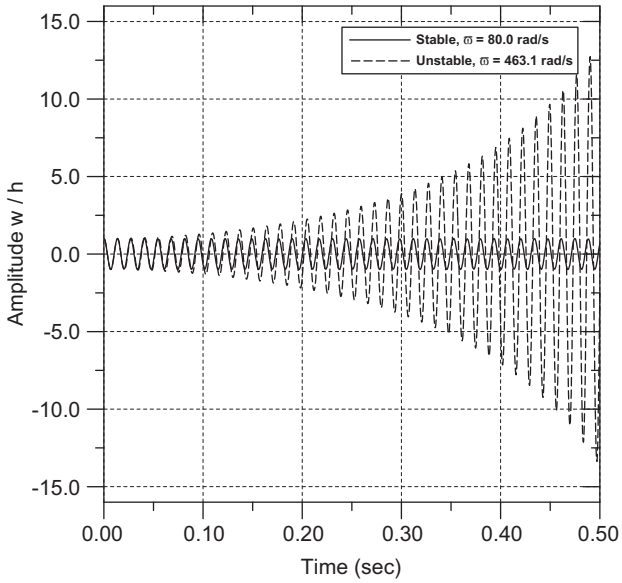

Fig. 12. The relationship of amplitude and time of the system ($k_1 = 0$, $h_t/h_l = 1.0$, $\Delta T = 3.0\,^{\circ}\mathrm{C}$ and $B_m = 0.3\,\mathrm{T}$) corresponding to different values of the excitation frequency ($\varpi = 80.0$ and $463.3\,\mathrm{rad/s}$, point B).

5. Conclusions

Based on the Hamilton's principle, the assumed mode, the Euler Bernoulli beam theory, and the Galerkin's method, the mechanical model of a bimaterial beam subjected to the thermal loads in an alternating transversal magnetic field with considerations of damping, the electromagnetic force, and torque is derived. For a bimaterial beam, the equation of motion and the solution of thermal effect are obtained by superposing certain fundamental linear elastic stress state. The results of the dynamic instability and transient vibrations of the bimaterial beam system are influenced by the following conditions and parameters: (1) the temperature increase ΔT; (2) the magnetic field $\mathbf{B}_m$; (3) the thickness ratio h_t/h_l; (4) the excitation frequency ϖ, (5) the dimensionless damping ratio k.

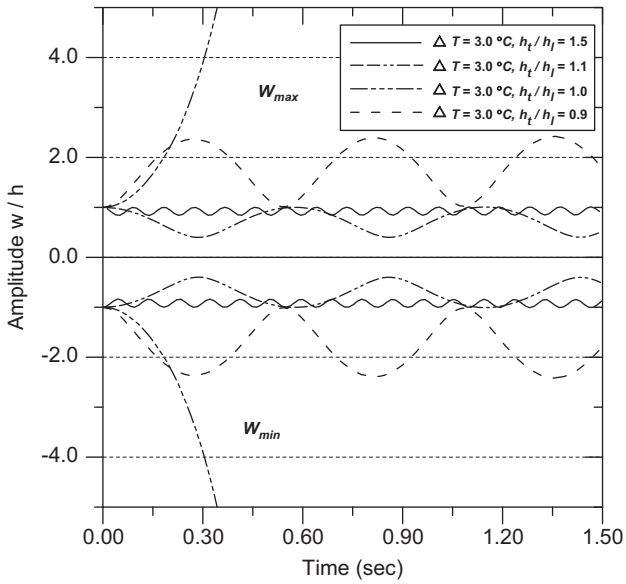

Fig. 13. The relationship of amplitude and time of the system ($k_1 = 0$, $\Delta T = 3.0\,^{\circ}\mathrm{C}$, $B_m = 0.3\,\mathrm{T}$, and $\varpi = 463.3\,\mathrm{rad/s}$) for the cases with different values of the thickness ratio.

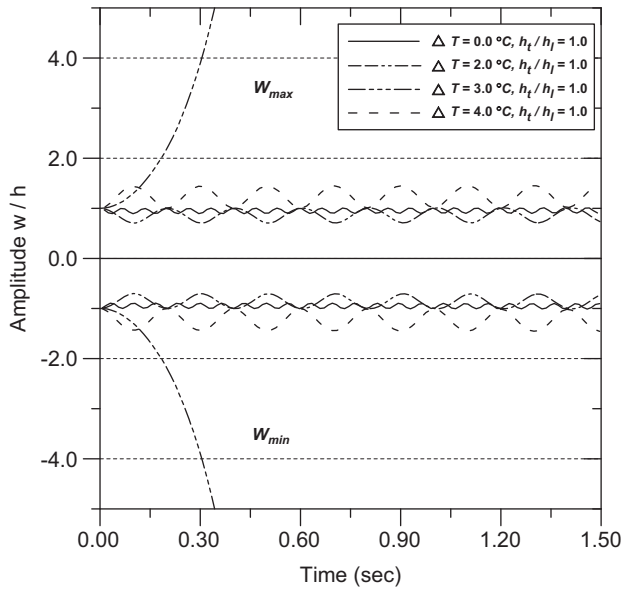

Fig. 14. The relationship of amplitude and time of the system ($k_1 = 0$, $h_t/h_l = 1.0$, $B_m = 0.3\,\mathrm{T}$, and $\varpi = 463.3\,\mathrm{rad/s}$) for the cases with different values of the temperature increase.

For the same thickness ratio, the results reveal that increasing either the magnetic field or the thermal load decreases the value of natural frequency of the system. Furthermore, increasing temperature shifts the region of dynamic instability to a lower value and produces a large variety of responses. Because of the double-layered bimaterial beam with different coefficients of linear thermal expansion in this study, the effect of thickness ratio on the dynamic instability region and transient vibration characteristic is obvious, and the results show that increasing the thickness ratio has the beneficial effect of increasing the value of natural frequency. When the excitation frequency ϖ is a constant, the transient vibration is obviously effected by the changes of the temperature increase and thickness ratio.

References

[1] T. Tagaki, J. Tani, Y. Matsubara, T. Mogi, Dynamic behavior of fusion structural components under strong magnetic fields, *Fusion Engineering and Design* 27 (1995) 481–489.
[2] Y.S. Shih, G.Y. Wu, J.S. Chen, Transient vibrations of a simply-supported beam with axial loads and transverse magnetic fields, *Mechanics of Structures and Machines* 26 (1998) 115–130.
[3] Y.H. Zhou, Y.W. Gao, X.J. Zheng, Q. Jiang, Buckling and post-buckling of a ferromagnetic beam-plate induced by magnetoelastic interactions, *International Journal of Non-linear Mechanics* 35 (2000) 1059–1065.
[4] X.J. Zheng, X.Z. Wang, Analysis of magnetoelastic interaction of rectangular ferromagnetic plates with nonlinear magnetization, *International Solids and Structures* 38 (2001) 8641–8865.
[5] X.J. Zheng, Y.H. Zhou, K. Miya, An analysis of variable magnetic damping of a cantilever beam-plate with coils in transverse magnetic fields, *Fusion Engineering and Design* 55 (2001) 457–465.
[6] E. Pan, P.R. Heyliger, Free vibrations of simply supported and multilayered magneto-electro-elastic plates, *Journal of Sound and Vibration* 252 (2002) 429–442.
[7] X. Zheng, J. Zhang, Y. Zhou, Dynamic stability of a cantilever conductive plate in transverse impulsive magnetic field, *International Journal of Solids and Structures* 42 (2005) 2417–2430.
[8] A.R. Annigeri, N. Ganesan, S. Swarnamani, Free vibrations of clamped–clamped magneto-electro-elastic cylindrical shells, *Journal of Sound and Vibration* 292 (2006) 300–314.
[9] A.R. Annigeri, N. Ganesan, S. Swarnamani, Free vibration behaviour of multiphase and layered magneto-electro-elastic beam, *Journal of Sound and Vibration* 299 (2007) 44–63.
[10] B. Pratiher, S.K. Dwivedy, Parametric instability of a cantilever beam with magnetic field and periodic axial load, *Journal of Sound and Vibration* 305 (2007) 904–917.
[11] A. Thorton, *Thermal Structures for Aerospace Applications*, AIAA Education Series, Reston, VA, 1996.
[12] P. Ribeiro, E. Manoach, The effect of temperature on the large amplitude vibrations of curved beams, *Journal of Sound and Vibration* 285 (2005) 1093–1107.
[13] J.W. Eischen, J.S. Everett, Thermal stress analysis of a bimaterial strip subject to an axial temperature gradient, *ASME, Journal of Electronic Packaging* 111 (1989) 282–288.
[14] A.P. Kfouri, H.D. Wong, Comparisons of theoretical and finite element stress analysis solutions for a bimaterial strip and plate subjected to thermal loading, *Fatigue and Fracture of Engineering Materials & Structures* 16 (1993) 1381–1395.
[15] F.C. Moon, Y.H. Pao, Magnetoelastic buckling of a thin plate, *ASME Journal of Applied Mechanics* 35 (1968) 53–58.
[16] F.C. Moon, Y.H. Pao, Vibration and dynamic instability of a beam-plate in a transverse magnetic field, *ASME Journal of Applied Mechanics* 36 (1969) 92–100.
[17] K. Miya, T. Takagi, Y. Ando, Finite element analysis of magnetoelastic buckling of a ferromagnetic beam-plate, *ASME Journal of Applied Mechanics* 47 (1980) 377–382.
[18] A.C. Eringen, Theory of electromagnetic elastic plates, *International Journal of Engineering Science* 27 (1989) 363–375.
[19] J.S. Lee, Destabilizing effect of magnetic damping in plate strip, *ASCE Journal of Engineering Mechanics* 118 (1992) 161–173.
[20] T. Tagaki, J. Tani, Y. Matsubara, T. Mogi, Dynamic behavior of fusion structural components under strong magnetic fields, *Fusion Engineering and Design* 27 (1995) 481–489.
[21] W. Yang, H. Pan, D. Zheng, Q. Cai, An energy method for analyzing magnetoelastic buckling and bending of ferromagnetic plates in static magnetic fields, *ASME, Journal of Applied Mechanics* 66 (1999) 913–917.
[22] G.Y. Wu, The analysis of dynamic instability and vibration motions of a pinned beam with transverse magnetic field and thermal loads, *Journal of Sound and Vibration* 284 (2005) 343–360.
[23] G.Y. Wu, The analysis of dynamic instability on the large amplitude vibrations of a beam with transverse magnetic fields and thermal loads, *Journal of Sound and Vibration* 302 (2007) 167–177.
[24] F. Ziegler, G. Rammerstorfer, Thermoelastic stability, in: R.B. Hetnarski (Ed.), *Thermal Stress*, Vol. III, Elsevier, Amsterdam, 1989.
[25] S.L. Lau, Y.K. Cheung, Amplitude incremental variational principle for nonlinear vibration of elastic systems, *ASME Journal of Applied Mechanics* 48 (1981) 959–964.
[26] S.L. Lau, Y.K. Cheung, S.Y. Wu, A variable parameter incrementation method for dynamic instability of linear and nonlinear systems, *ASME Journal of Applied Mechanics* 49 (1982) 849–853.
[27] S.L. Lau, S.W. Yuen, Solution diagram of non-linear dynamic systems by the IHB method, *Journal of Sound and Vibration* 167 (1993) 303–316.
[28] V.V. Bolotin, *The Dynamic Stability of Elastic System*, Holden-Day, San Francisco, 1964.